Chin. Geogra. Sci. 2013 Vol. 23 No. 1 pp. 101–112
doi: 10.1007/s11769-012-0580-7

Springer Science Press
www.springerlink.com/content/1002-0063

Pattern Dynamics of Thermal-environment Effect During Urbanization: A Case Study in Shenzhen City, China

XIE Miaomiao[1], WANG Yanglin[2], FU Meichen[1], ZHANG Dingxuan[1]

(1. *School of Land Science and Technology*, *China University of Geosciences*, *Beijing* 100083, *China*; 2. *College of Urban and Environmental Sciences*, *Peking University*, *Beijing* 100871, *China*)

Abstract: The thermal-environment effect exists in the field of rapid urbanization. It has adverse effects on the urban atmosphere, regional climate, energy consumption, and public health. Shenzhen, a representative of rapidly urbanizing cities in China, was selected as a case for pattern dynamics analysis of the thermal environment. The surface temperature was acquired from the thermal infrared data of Landsat TM and ETM+ images in 1986, 1995, and 2005 by Jiménez-Muñoz and Sobrino′s generalized single-channel method, which was used in assessing the distribution and spatial patterns of the thermal environment. The relative thermal environment curve (RTC) was combined with Moran′s I analysis to assess the pattern dynamics of the thermal environment in different urbanization periods. Moran′s I index and the RTC represent a process of aggregation-fragmentation-aggregation, which shows the aggregation pattern of a decrease during the rapid urbanization period and then an increase during the steady urbanization period. High-temperature areas gradually expanded to a uniform and scattered distribution in the rapid urbanization period; while the high thermal-environment effect was gradually transformed into a steady spatial pattern in the stable urbanization period. To characterize the increasing development in this multiple-center city, we chose profiles along an urban-development axis. The results suggest that heat islands have expanded from internal urban to external urban areas. Four profiles were obtained showing differences in shape due to spatial differences in the process of development.
Keywords: thermal environment; spatial pattern; remote sensing; urbanization; Shenzhen City

Citation: Xie Miaomiao, Wang Yanglin, Fu Meichen, Zhang Dingxuan, 2013. Pattern dynamics of thermal-environment effect during urbanization: A case study in Shenzhen City, China. *Chinese Geographical Science*, 23(1): 101–112. doi: 10.1007/s11769-012-0580-7

1 Introduction

The environmental problems resulting from rapid urbanization will affect more than half of the world′s population (Demographia, 2010; Imhoff *et al*., 2010). Urban climate change is one of the important environmental problems caused by urbanization. Howard (1833) proposed the concept of the urban heat island (UHI) to describe the phenomenon of high temperature of urban centers accompanying the urbanization process. In areas of rapid urbanization, temperature is distributed as an urban heat ′archipelago′ instead of a ′island′ because of landscape fragmentation (Buyantuyev and Wu, 2010). Therefore, we use the concept of the thermal-environment effect for assessing all of the thermal characteristics of a city. The thermal environment effect, a typical environmental effect, is the temperature response to human activities in certain urban areas.

The spatial pattern of the thermal environment is an indicator of urban ecosystems influenced by urbanization, and it is also an activator of other environmental problems in urban regions. The pattern of the thermal environment also affects regional climate (Grimm *et al*., 2008), energy consumption (Coudert *et al*., 2008), public health and the urban atmosphere. A temperature increase contributes to regional climate changes with the rapid expansion of urban heat islands (Roth *et al*., 1989; Saaroni *et al*., 2000). High temperatures cause lower

Received date: 2012-01-30; accepted date: 2012-06-04
Foundation item: Under the auspices of National Natural Science Foundation of China (No. 41101175, 40635028)
Corresponding author: XIE Miaomiao. E-mail: xiemiaomiao@cugb.edu.cn

atmospheric pressures in urban areas than in rural areas, resulting in polluted air reflux to urban areas (Voogt and Oke, 2003; Yuan and Bauer, 2007). The probability of prevalent diseases, respiratory illnesses, and cardiovascular mortalities increases with temperature rises in urban areas (Patz *et al*., 2005). The most serious consequence is that the expansion of areas with high temperature and a resulting increase of energy consumption cause a spiraling problem. For example, high temperature leads to widespread use of air conditioners to reduce the indoor temperature (Rosenfeld *et al*., 1995; Weng and Yang, 2004; Chang *et al*., 2007). An increase of 1°C in summer temperature may result in a 6% rise in electricity consumption due to air conditioning (Chang *et al*., 2007).

Surface temperature measurements by remote sensing are appropriate for the study of the pattern dynamics of thermal-environment effects because they have a higher spatial resolution than *in situ* air temperature (Voogt, 2002; Imhoff *et al*., 2010). Especially in the heterogeneous urban landscape, surface temperatures derived from remote sensing data are more sensitive to surface characteristics (Voogt and Oke, 2003; Nichol and Wong, 2005). Pattern dynamics analysis based on remote sensing includes temperature gradients and dynamics in both spatial and temporal dimensions.

Temperature gradient patterns from urban center to rural areas are good examples for depicting the spatial variation of the urban thermal environment. Following the research approach used in urban climatology, the regular approach to describing gradient patterns of the thermal environment across urban area should be profile analysis (Carlson *et al*., 1994; Yue and Xu, 2008). In previous studies, the direction of profiles was from urban center to eight points of the compass (Streutker, 2002; Weng, 2003; Zhang *et al*., 2006). However, multiple urban centers have been formed instead of a single center in group-development cities. Fragmented landscapes make heat spots as multiple-island, archipelago distributions in such cities (Buyantuyev and Wu, 2010). Profiles from urban center to suburb can not represent urban development gradients of multiple-center cities. Instead, an urban-development axis was applied for selecting profiles in multiple-center cities. By comparing the shape and structure of surface temperature profiles, the peak and valley can be found, and the differences between the urban area and the suburban area can be derived.

The pattern dynamics of the thermal environment can be evaluated by landscape metrics. The results show that the thermal environment acquires an uneven distribution, a fragmentation pattern, and a complex texture with urban expansion (Chen *et al*., 2002; Weng, 2003). Before the landscape-metrics calculations, thermal environments are classified by temperature degree or land-use types. Subjective classification and descriptions have a significant influence on landscape metrics (Peng *et al*., 2007). To avoid the influence of subjective classification on landscape metrics, a geo-statistics method for continuous data is suitable for assessing spatial-pattern dynamics of the thermal environment. A Gaussian surface and non-parametric model have taken a regional perspective on the thermal environment deriving from the magnitude and the location of urban heat islands (Streutker, 2003; Rajasekar and Weng, 2009). However, they are generalizations and up-scaled methods for describing spatial patterns of the thermal environment that cause information loss.

Shenzhen, the first special economic zone in China, which has experienced rapid urban expansion and steady development since 1986 (Wang, 2003), is taken as the case study area. The urbanization process leads to concentration of population and economic activity. From a geographic perspective, the aggregation of economic activities is followed by spatial expansion of urban areas. At the same time, spatial expansion causes fragmentation in the urban landscape (Grimm *et al*., 2008). Derived from the aggregation process of human activities and landscape fragmentation, the spatial patterns of the thermal environment vary in different urbanization periods. Our interest is in the pattern dynamics of the thermal-environment effect during different urbanization periods. In this study, to avoid subjectivity and information loss, we develop a method of spatial pattern analysis involving temperature values in every pixel. This approach is used to describe spatial and temporal patterns of the thermal environment based on a geo-statistics method. We use thermal dynamics curves combined with spatial autocorrelation analysis to characterize the pattern dynamics of the thermal environment under the influence of human activity aggregation and urban sprawl in different urbanization periods.

2 Materials and Methods

2.1 Study area and data sources

Shenzhen is located on the Zhujiang (Pearl) River Delta

in the southeastern China. It has an area of 195 284 ha and includes Futian District, Luohu District, Nanshan District, Yantian District, Bao′an District, and Longgang District (Fig. 1). Shenzhen City has a southern subtropical monsoon climate, a mean annual temperature of 22.4°C, and a mean annual rainfall of 1948 mm.

As economy development has proceeded rapidly, Shenzhen has changed from a traditional agricultural region to a rapidly-developing urban region and has experienced rapid urbanization over the past two decades. As shown in previous studies, approximately 39.3% of the total land area was urban in 2005, an increase from only 3.06% in 1986 (Li *et al*., 2005).

Urbanization in Shenzhen has passed through three phases. It was initiated from 1978 to 1986, which was the primary stage of urbanization. In the second period, 1986–1995, the development of urbanization became very rapid. From 1995 to the present, the tempo of urbanization has slowed down, and density increase in urban areas has become the main result of urbanization rather than spatial expansion (Wang, 2003). To better analyze the spatial dynamics of urbanization in different periods, we chose 1986, 1995, and 2005 as the study period. The data source for the study was Landsat TM images acquired in the winters of 1986, 1995, and 2005 (path 121/row 44 and path 122/row 44). All images were acquired in winter under sunny and windless weather conditions, providing a steady atmospheric condition favorable for thermal-environment studies.

2.2 Surface temperature retrieval

According to the climate characteristics and availability of parameters in the study area, we selected the generalized single-channel method developed by Jiménez-Muñoz and Sobrino (2003) for surface temperature retrieval. This method requires the total water vapor as the parameter (Jiménez-muñoz and Sobrino, 2006).

The first step was to calculate the brightness temperature T_b transferred from digital number (DN) data using the following formula based on Plank′s function of radiation (Schott and Volchok, 1985; Wukelic *et al*., 1989):

$$L_\lambda = GAINS \times DN + BIASES \tag{1}$$

$$T_b = \frac{K_2}{\ln(\frac{K_1}{L_\lambda} + 1)} \tag{2}$$

where L_λ is the at-sensor radiance calculated by *DN*; *DN* is the digital number of the infrared thermal band of Landsat TM 5; *GAINS* and *BLASES* values are derived from the head files of the images; K_1 and K_2 are calibration constants. K_1 = 607.66 W/(m^2·sr·μm), and K_2 = 1260.56 K. The unit of T_b is Kelvin (K).

Surface temperature (T_s) is retrieved by the generalized single-channel method using parameters including at-sensor radiance L_λ, brightness temperature T_b, radiation wavelength (11.457 μm for TIR data) and the emissivity (Jiménez-Muñoz and Sobrino, 2003). The emissivity can be calculated by the NDVI method (Valor and Caselles, 1996; Jiménez-muñoz and Sobrino, 2006). The parameters in the generalized single-channel method are calculated using the functions for total atmospheric water vapor content derived from *in situ* meteorological data (Jiménez-Muñoz and Sobrino, 2003; Jiménez-muñoz and Sobrino, 2006; Li *et al*., 2010).

Splicing of the two images in each year was implemented by following the normalization of temperature

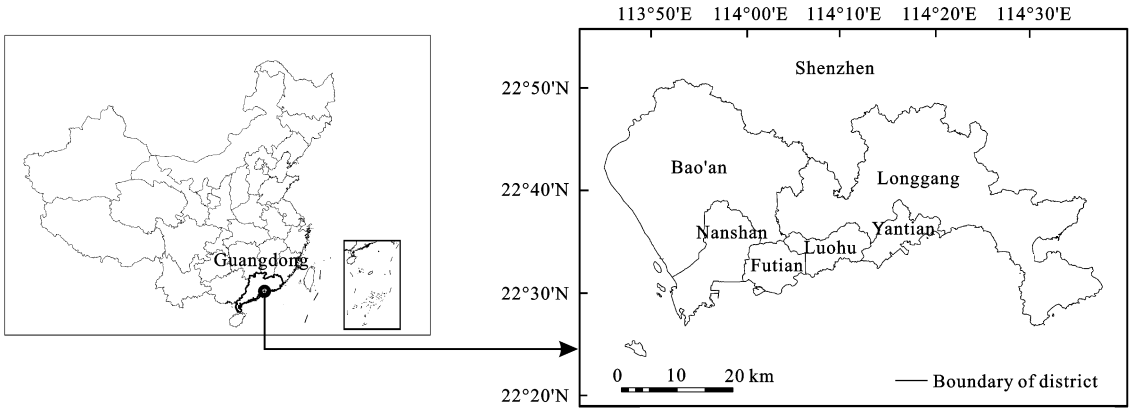

Fig. 1 Location and districts of Shenzhen

differences in overlap areas of the two images. All images were geometrically rectified to the local coordinate system of Shenzhen with a pixel error by 50 ground control points, which were symmetrically distributed across the image. The regression of surface temperature and *in situ* 0-cm soil temperature measurements indicates that surface temperature values are consistent with *in situ* surface temperature, with R^2 greater than 0.95. In addition, Jiménez-muñoz and Sobrino (2006) reported that the error of this method came from the error of water vapor, with average error between 0.3 K and 0.8 K. Using the evaluation method proposed by Qin *et al*. (2003), based on water vapor, the systematical error is 0.6 K.

2.3 Spatial autocorrelation analysis and relative thermal environment curves

Spatial autocorrelation is considered to be the first law in geography (Tobler, 1970), which means that the influencing function between two nearby phenomena is larger than that between two distant objects (Wang, 2006). It is suitable for spatial analysis of continuous data such as temperature, elevation, soil moisture. Spatial autocorrelation indices include Moran′s I index, Geary′s C index, and the Getis index (Moran, 1948; Geary, 1954; Getis and Ord, 1992). Moran′s I index was chosen for the spatial autocorrelation analysis of surface temperature to assess spatial patterns of the thermal environment in each year of the study. Moran′s I value is between –1 and 1. The more aggregation exists in the spatial pattern, the larger Moran′s I value is. When Moran′s I is lower than 0, it means a negative correlation in the spatial patterns. When there is no spatial correlation, the Moran′s I value is 0. When the value is larger than 0, the autocorrelation is positive.

The degree of spatial autocorrelation is used to characterize the aggregation pattern of high-temperature zones (Song *et al*., 2007), while it does not illustrate the temperature value with an aggregation pattern. For solving the problems, we analyzed the spatial dynamics of the thermal environment by a modified method based on the relative altitude curve (RAC). The RAC is an accumulative area curve that can describe the spatial aggregative pattern of altitude (Zhang and Yang, 1991). Relative altitude can be calculated as (*h*–*b*) / (*H*–*b*), where *h* is the elevation of a certain pixel; *b* is the minimum elevation in the watershed; and *H* is the maximum elevation in the watershed. When the value ranges of the vertical axis are the same between watersheds, it is better for comparison. The horizontal axis is the cumulative-percentage area above the corresponding vertical value. By the statistics of the cumulative-percentage area above certain evaluation values, the RAC can be formed. The shape of the RAC indicates different landform situations, so it supplies the reference for quantitative analysis by the Davis landform theory. If the curve is similar to a straight line, it indicates that the landform in the watershed is closer to the erosion basis (Zhang and Yang, 1991).

Proceeding from the analysis approach of the RAC, we now define the relative thermal environment index (*RT*) by Equation (3), which represents the location of a certain pixel on a temperature array.

$$RT = (T_i - T_{\min}) / (T_{\max} - T_{\min}) \quad (3)$$

where T_i is the temperature value of pixel *I*; $T_{\max}$ is the maximum temperature of the whole study area; and $T_{\min}$ is the minimum temperature. If *RT* is 1, it means the surface temperature of this pixel is on the greatest level in the study area. If *RT* is 0, it is on the lowest level. The first step is to use the Visual Basic editor in ArcGIS 9.2 to read the surface-temperature value of each pixel and to calculate *RT*. The second step is to count the numbers of every *RT* value. The third step is descendant sorting of the *RT* values of every pixel and calculation of the cumulative-percentage area of every value. Finally, the relative thermal environment curves (RTCs) can be drawn by scatters of *RT* values and cumulative-percentage-area values. Curve shape suggests the aggregation degree of the thermal environment. The larger the curvature, the greater the aggregative pattern of the thermal environment. The distance between curves and the X-axis determines the level at which the thermal-environment aggregation occurs. When the distance is small, aggregation appears on the level of high surface temperature.

2.4 Distribution index of relative thermal environment

We now introduce the distribution index (*DI*) to characterize the effect of each district on the thermal environment. The *DI* represents the contribution of each district to the overall thermal-environment effects:

$$DI = \frac{S_{ij}}{S_i} \Big/ \frac{S_j}{S} \quad (4)$$

where S_{ij} is the area with *RT* greater than 50% in district *j*; S_i is the area with *RT* greater than 50% in Shenzhen; S_j is the area of district *j*; *S* is the city′s total area.

If the *DI* is greater than 1, it indicates that the district contributes more than average to the thermal-environment effects. If *DI* is lower than 1, it indicates that the district contributes less than average to the thermal-environment effects. If *DI* equals 1, it shows that the thermal-environment effects of district *j* are similar to those of the whole level.

2.5 Profile selection for spatial distribution analysis

The spatial distribution of a thermal environment represents thermal variations as spatial location changes. According to traditional aerographic methods, profile analysis and isotherms are often used to measure the spatial distribution of thermal-environment effects (Bornstein, 1968; Saaroni *et al*., 2000). The former is used to represent the temperature variation from city center to suburbs. The profile selection method is based on the analysis results of thermal variation (Song *et al*., 2007). Generally, for a single-center city, such as the Twin City in the USA and Shanghai in China, the preferred profile runs from the city center to the suburbs (Chen *et al*., 2002; Yuan and Bauer, 2007; Yue and Xu, 2007). For multiple-center cities, the method of vertical-horizontal cross and equiangular distribution provide another regular method to locate profiles (Zhang *et al*., 2006; Xie *et al*., 2008; Yue and Xu, 2008).

However, in multiple-center cities, urban landscapes expand from several cores to their surrounding areas. The above-mentioned profiles are not suitable for describing urban development gradients and urbanization dynamics in multiple-center cities. Urban expansion in Shenzhen is characterized by group development with multiple urban centers. Urban landscapes expand along four development axes: west, middle, east, and south. (Wang, 2003) (Fig. 2). To reflect the spatial variation of urban development, we select profiles based on development axes as to analyze the thermal environment distribution. The west profile expands from the urban semi-center in Nanshan to western industry zones of Bao′an along the west development axis. The surroundings of the west profile underwent industrial development earlier. The middle profile extends from the urban center to the storage and industry zones including Buji, Guanlan, and Pinghu Streets. The east profile runs from the urban center to the center of Longgang along east development axis. Areas around the east profile have developed later than other areas. The south profile follows the development axis in the special economic zone (SEZ), which passes through industry centers in Zhaoshang and Nantou streets, the High-tech Industrial Park, and the storage center in Nanshan, the administrative and business center in Futian, and then to Yantian Port and Yantian.

3 Results

3.1 Pattern dynamics of thermal environment

High Moran′s I index values of surface temperature indicate that the urban thermal environment is positively auto-correlated (Table 1). Surface temperature is easily influenced by nearby pixels. Moran′s I indices at differ-

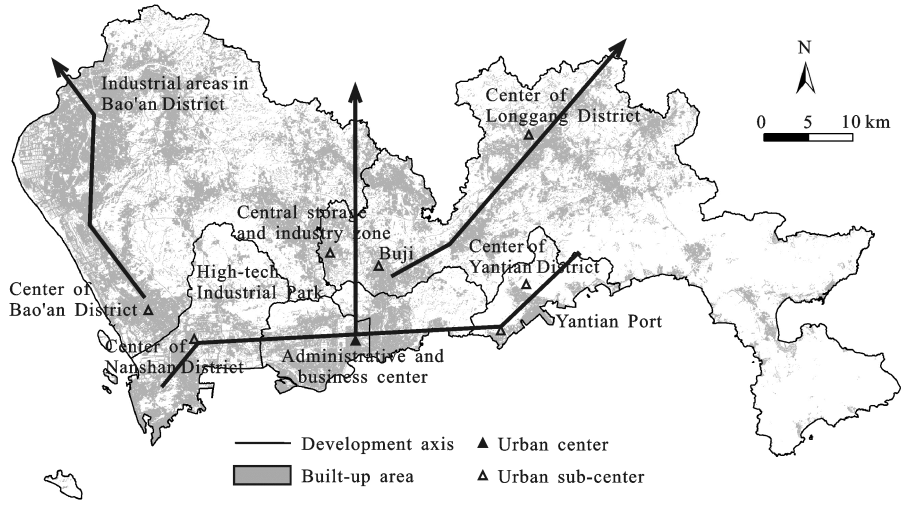

Fig. 2 Urban spatial configuration of Shenzhen and profiles

ent resolutions show that the strength of the correlation decreases as the scale increases. Spatial correlations at 30-m resolution are the strongest. On every scale, the spatial correlation of the thermal environment in 1986 was the strongest one. On the scale of 120 m, the Moran′s I value in 1986 was 0.86. This result indicates that the spatial distribution of surface temperature in 1986 is the most aggregative pattern of the urbanization period. The second-largest value was in 2005. The least spatial correlation occurred in 1995. The values of Moran′s I index indicate that the aggregation pattern of the thermal-environment effect includes first a decrease in the rapid urbanization period and then an increase in the steady urbanization period.

Relative thermal environment curves had similar shapes in 1986, 1995, and 2005, but they had great differences in distribution location, curvature, and the distance to the X-axis (Fig. 3). In this paper, the median value was chosen as the standard for comparison. The percent of accumulative area above the median value varied in the three periods.

The curvature of the RTC represents the aggregation degree of the thermal environment. For the curve of 1995, the major pixels were distributed on the nearby median value of surface temperature, and the angle between the curve and X-axis was smaller than that in 1986 and 2005. In 1986 and 2005, the major pixels were distributed on the two extremes of the thermal environment values. It shows that the curve in 1995 represents more flat than curves in 1986 and 2005. The spatial patterns of the thermal environment in 1986 and 2005 were more aggregative than that in 1995.

The location and distance to the X-axis of curves in the coordinate system show the position where aggregation occurs. The curve for 1986 was located on the bottom of the coordinate system. The curve for 1995 was located between the curves for 1986 and 2005. The curve for 2005 is located on the top. According to the curve for 1986, less than 10% of the area has *RT* values greater than 0.5. The areas with high surface temperature are limited to the initial stage of urbanization, and the pixels aggregate on the level of low surface temperature. The areas with *RT* above 0.5 have increased rapidly to 50% from 1986 to 1995. During this period, the area having a *RT* value greater than 0.4 grew to 80%. The urban heat island effect has been rather significant in Shenzhen. In 2005, nearly 80% of the area had *RT* values above 0.5. The thermal-environment effect aggregates on the greatest level of surface temperature in the steady urbanization period.

Table 1 Moran′s I values of surface temperature on different scales

Year	30 m	60 m	120 m
1986	0.98	0.93	0.86
1995	0.97	0.92	0.83
2005	0.98	0.85	0.85

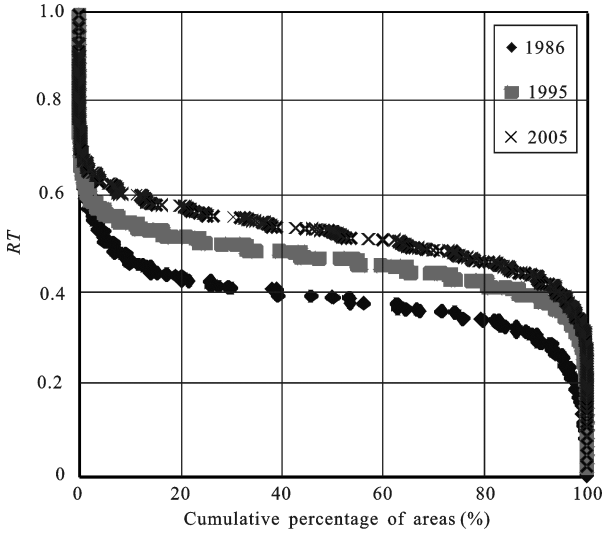

Fig. 3 Relative thermal environment curve of urban landscape

3.2 Spatial variation of thermal environment among districts

The *DI* for each district in 1986, 1995 and 2005 was calculated (Fig. 4). The differences of *DI* values among the six districts became smaller during urbanization. In 1986, the *DI* values ranged from 0.03 to 4.58. Yantian District contributed most to the thermal-environment effects. The *DI* values of Futian, Nanshan and Bao′an districts were very low. In 1995, with the spread of ur-

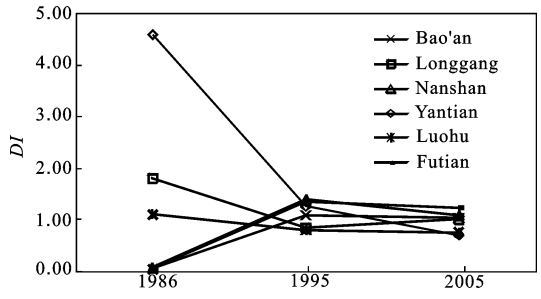

Fig. 4 Distribution index of thermal environment effect in each district

ban heat islands, the contribution of each district to the thermal-environment effects became much more similar than they were in 1986. The range of *DI* values in 2005 was 0.70 to 1.22. Futian contributed most to the thermal environment.

The *DI* values help to explain the thermal heterogeneity that characterizes each district in different urbanization periods. In 1986, Bao′an District contributed little to the thermal environment in Shenzhen. Compared to the initial one, the *DI* values in 1995 and 2005 were higher than 1, which indicated that Bao′an became an area with high thermal-environment effects. Longgang District showed a trend that was opposite to that of Bao′an District. In 1986, the *DI* of Longgang was higher than 1. After Shenzhen′s reforesting in the 1990s, the contribution of Longgang in 1995 and 2005 were apparently smaller than that in 1986. Luohu, the initial downtown of Shenzhen, showed a decreasing trend of the *DI*. In 1995 and 2005, Luohu District contributed negatively to the high thermal-environment effects of Shenzhen. The trends of Nanshan and Futian districts were similar. In the initial stage of urbanization, these two districts made limited contribution to the urban thermal environment. The *DI* values increased greatly during the urbanization period, becoming greater than 1. The changes of the *DI* values in Yantian were the largest among the six districts. In 1986, Yantian contributed greatly to the increasing thermal environment of Shenzhen. After the 1990s, the *DI* value decreased to 1.24 and then became lower than 1 in 2005, which indicates a negative contribution to the whole thermal environment.

3.3 Spatial variation of thermal environment along profiles

Temperature values on the four profiles were obtained with the profile tools of ArcGIS 9.2. Spatial variations are very heterogeneous, as indicated by the extreme values, the slope of the trend line, and the curvature of four profiles (Fig. 5).

The thermal environment in Shenzhen changed during the urbanization process from 1986 to 2005. The profiles suggest that the locations of high temperature areas changed. There were only a few high-temperature patches in the city center. After 1986, high-temperature patches expanded to every district of Shenzhen. On the west profile, middle profile and east profile, the highest temperature values in 2005 were much higher than that in 1986 (Fig. 5). For the south profile, the top of the curve in 1986 was higher than that in 2005, in contrast to to the other profiles. In 1986, high-temperature areas were closely related to bare land on the hills in Yantian and internal urban areas in Futian and Luohu.

The slope of the trend line shows temperature changing from the urban core to Bao′an and Longgang districts (Fig. 5). Along with the west profile curve, urban interior is warmer than the exterior in 1986, while the opposite trend characterizes the urbanization period. The shapes of the middle and east profiles showed few changes during the urbanization process from 1986 to 2005. The middle profiles showed that the surface temperature in the urban interior was higher than that in the exterior. The east profile showed the surface temperature increasing with large amplitude from the urban center to Longgang. The south profile shows a significant wave with an ascending trend from Nanshan to Yantian in 1986 and a reversal of the trend in 2005.

Though the temperature trend lines show spatial and temporal heterogeneity between profiles, the peak values showed a homogenous trend with higher temperatures in 2005 than that in 1986. In 2005, the west profile showed two peaks corresponding to the urban interior and Industrial areas in Shajing-Songgang of Bao′an. There were two obvious peaks corresponding to Shenzhen Dump and Yinhu Passenger Station on the east profile, where the surface radiation was high. The peak values of the south profile occured in Nanshan and Futian districts in 2005. In 1986, the temperature variation in Yantian District was the greatest: temperature peak and valley values both appeared. The low temperature of the valley was caused by sea temperature before sea reclamation. The high temperature of the peak was caused by the high reflectance of the bare rock on the mountain. Since the afforestation by aerial seeding in the 1990s, mountains in Yantian District have been covered with vegetation. Because of this, the temperature in Yantian decreased from 1995 to 2005, and it is clearly lower than it is in other districts. The peak value in Yantian District in 2005 was located in Yantian Port.

4 Discussion

Urbanization is the consequence of people and non-agricultural activities aggregating in urban centers, and it also represents a spatial expansion of the urban land-

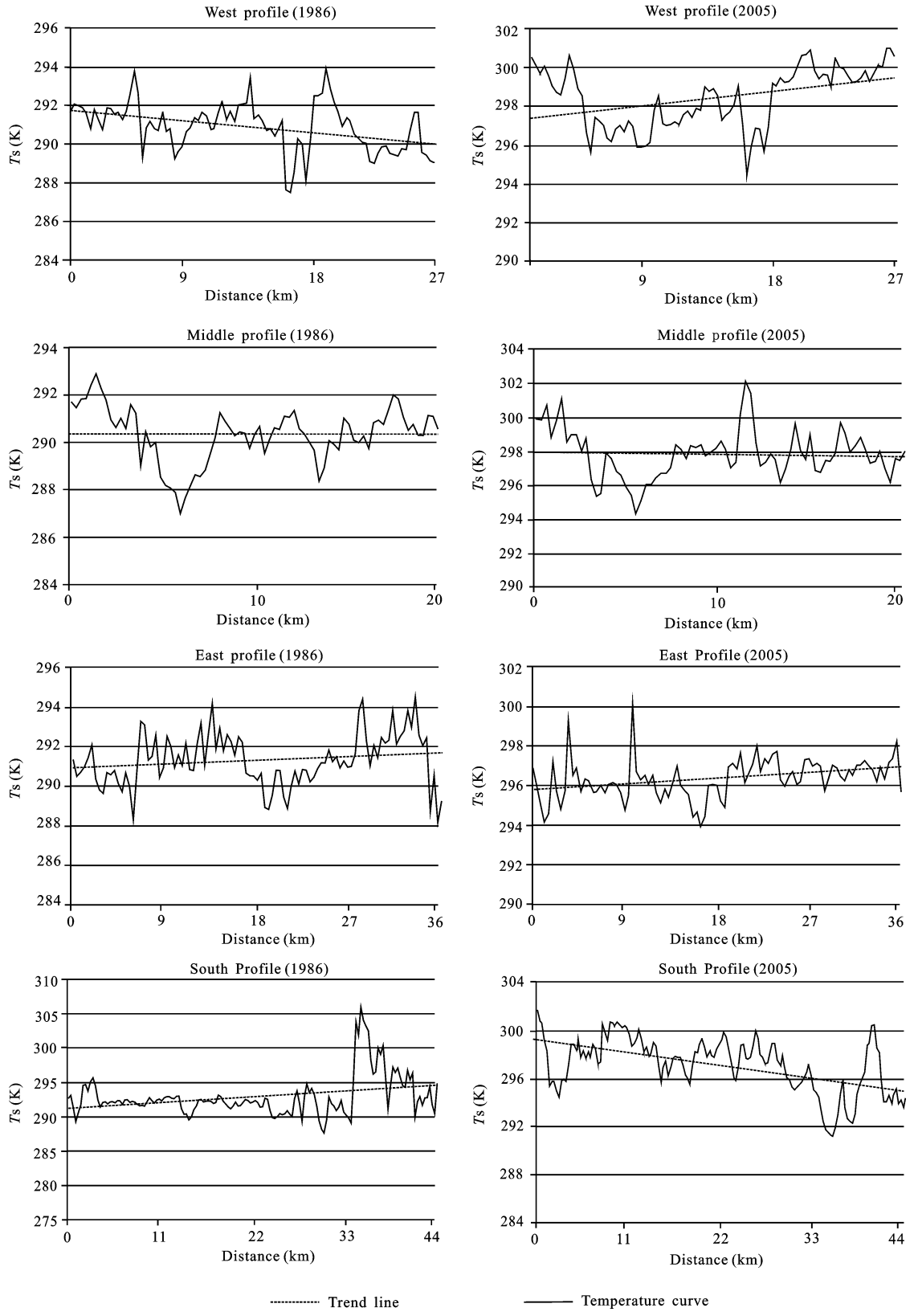

Fig. 5 Profiles of thermal-environment effects in Shenzhen

scape (Zhou, 1995). Zhou (1995) has argued that population aggregation is the main driving force in the early urbanization period, while the centrifugal power of population and economic activities is the main driving

force in the late period. In addition, the ecological effects can be varied under different urbanization characteristics and phases. The present study focused on the spatio-temporal patterns of the thermal-environment effect under various driving forces in different urbanization phases in Shenzhen.

4.1 Spatial patterns and process of thermal environment

In contrast to focusing on the location and magnitude of UHIs within a short period, as done in previous studies (Yuan and Bauer, 2007; Rajasekar and Weng, 2009), we find that the patterns of the thermal environment present an aggregation-fragmentation-aggregation process along with rapid-steady urbanization periods. Our study resulted in two breakthroughs for assessing the spatial pattern dynamics of the thermal environment. Firstly, some quantitative methods for characterizing UHI patterns such as a non-parametric model and a Gaussian model are generalized methods that smooth the fragmentation patterns of the thermal environment (Streutker, 2002; 2003; Rajasekar and Weng, 2009). In a heterogeneous urban landscape, these methods may lose some information. We developed a relative-thermal-environment curve method involving all pixels of the study area in the analysis. Secondly, many studies on the temporal changes of the thermal environment have focused on seasonal or short-period changes (Streutker, 2002; Weng *et al*., 2008). Our study focused on the description of thermal-environment patterns along urban-rural gradients in different urbanization stages. Shenzhen, as the case study, experienced a relatively integral urbanizing process, and it is appropriate for thermal-environment studies in different urbanization periods. Similar weather conditions are a precondition of comparability for long-term pattern dynamics. Data with similar weather characteristics in the same season were chosen, and the relative thermal environment index was adopted for comparing the thermal environment in different years. The RTC provides a comparison method to evaluate spatial patterns in different urbanization periods by the distribution, the curvature, and the distance to the X-axis. This approach can avoid the subjectivity of classification methods for describing spatial patterns of the thermal environment. In addition, it can compare different cities after normalization of surface temperature. In this way, we can deduce the urban characteristics and thermal patterns in different cities. This will also be the emphasis in our future research.

The changes of Moran′s I indices from 1986 to 2005 showed that the spatial pattern of the thermal environment is aggregative in the initial stage of urbanization, and the spatial pattern then gradually became scattered in the rapid-urbanization stage. In the steady-urbanization stage, surface temperature distribution became aggregative again. The results of RTC were consistent with the aggregation changes derived from the autocorrelation analysis. Integration of spatial autocorrelation analysis and the curves of relative thermal environment showed that pixels gathered on the low-thermal-effect level in the initial urbanization period. In the rapid urbanization stage, along with the rapid expansion of the urban landscape, high-temperature centers rapidly spread into fragmentation patterns. The areas with high relative thermal-environment effect had become the main part of Shenzhen. In the late stage of urbanization, pixels with high temperature aggregated around the previous hotspots. Therefore, RTC in 2005 represented an aggregation pattern with high values (Fig. 3).

The results of this study suggest some new perspectives for better understanding of urban ecology and environment. The spatial pattern of the thermal environment is important for studies of urban ecology and environment. Taking the influence of the thermal environment on atmospheric patterns as an example, atmospheric pressure becomes lower when surface temperature increases. As a consequence, pollutants can not diffuse, and there is a deterioration of air quality in the urban area (Voogt and Oke, 2003; Yuan and Bauer, 2007). During the steady urbanization period in Shenzhen, multiple heat islands corresponded to multiple pollutant centers. If the city continues to expand, the contaminant centers will gradually form into very large contiguous areas that will greatly threaten the urban environment and the livability of the city.

4.2 Expansion of high-temperature areas with urban growth

By combining the results of this study with others (Amiri *et al*., 2009), it can be concluded that high-temperature areas grow along with the expansion of the urban landscape. Trend lines of profiles and DI values show an increasing trend from rural areas to urban cores, especially during the rapid urbanization period around

the west profile. Peak values of profiles indicate that high temperature areas have changed with urban expansion. After the Reform and Opening Policy in China in 1978, the SEZ in Shenzhen obtained the most preferential economic policy. Therefore, urbanization expanded earlier in the SEZ than outside the SEZ. Luohu and Futian districts were the earliest business, cultural, and administration centers of Shenzhen. In 1986, peak values on the middle and west profiles corresponded to Luohu and Futian districts (Fig. 5). Then Nanshan District developed as a high-tech industrial center of Shenzhen, and Bao′an District developed rapidly after 1995 as an industrial area. Therefore, an increase in surface temperature in Nanshan and Bao′an districts appeared on the west profile. The storage center and residential areas with low building density in the middle profile resulted in a cooler surface temperature than that in the culture and business centers.

However, the profiles showed that surface temperature was heterogeneous in urban areas because of different land-use types and human activities (Yue and Xu, 2008; Imhoff *et al*., 2010). Complex urban structures with fragmental and diverse landscapes are reflected more obviously in multiple-center cities (Buyantuyev and Wu, 2010). A single heat island is divided into fragmental patches by urban processes. That is why the concept of an urban heat archipelago is proposed instead of an urban heat island (Buyantuyev and Wu, 2010). Some cities, such as the Phoenix metropolitan region, lacking a mature urban downtown are also best represented as multiple islands (Golden, 2004; Buyantuyev and Wu, 2010). Profiles in this study represent fluctuations in both internal urban and external urban properties. Heterogeneity is caused by landscape diversity in urban areas, such as valley values in profiles corresponding to rivers, ponds, lakes, or forests, and peak values in profiles corresponding to industrial land, CBD, transportation centers, or barren land. Another causative factor is the influence of albedo. In the daytime, the thermal environment is influenced by complex factors including moisture, shade, and other thermal properties (Nichol, 2009). The combination of day-time and night-time thermal remote-sensing data to determine the causal mechanism would be a fruitful topic of further study in multiple-center cities.

5 Conclusions

The urban thermal environment is important for understanding the influences of urbanization on the urban ecosystem and environment. The study of spatial-pattern dynamics of the thermal environment describes the trajectory of thermal changes during different urbanization periods and is instructive for policymakers seeking to mitigate urban heat-island effects.

Based on a combination of spatial autocorrelation analysis and the relative thermal environment curve method, the effect of urbanization on the thermal environment in Shenzhen can be summarized as follows: high-temperature areas expanded gradually to uniform and scattered distributions in the rapid urbanization period, while in the stable urbanization period, areas with high thermal-environment effect gradually formed into a steadily aggregative spatial pattern. For multi-center cities, the urban-development axis provides an approach to the selection of profiles. These profiles reflect the expansion of heat islands from internal urban to external urban in their spatial distributions. Four profiles were selected to represent various shapes determined by spatial differences in the development process. In the rapid urbanization period, controlling the spread of urban heat islands is the key to minimizing urban climate change and to prevent non-heat-island areas from becoming heat islands. In the steady urbanization period, the control of initial urban heat islands has the benefit of decreasing UHI intensity, which can avoid temperature increases of the initial heat islands.

Acknowledgement

We appreciate Professor Zhao Xinyi for providing the meteorological data, and also appreciate Dr. Zeng Xiangkun for perfecting the figure.

References

Amiri R, Weng Q, Alimohammadi A *et al*., 2009. Spatial-temporal dynamics of land surface temperature in relation to fractional vegetation cover and land use/cover in the Tabriz urban area, Iran. *Remote Sensing of Environment*, 113(12): 2606–2617. doi: 10.1016/j.rse.2009.07.021

Bornstein R D, 1968. Observations of the urban heat island effect in New York City. *Journal of Applied Meteorology*, 7(4): 575–582.

Buyantuyev A, Wu J, 2010. Urban heat islands and landscape heterogeneity: Linking spatiotemporal variations in surface temperatures to land-cover and socioeconomic patterns. *Landscape Ecology*, 25(1): 17–33. doi: 10.1007/s10980-009-9402-4

Carlson T N, Gillies R R, Perry E M, 1994. A method to make use

thermal infrared temperature and NDVI measurements to infer surface soil water content and fractional vegetation cover. *Remote Sensing Review*, 9(1–2): 161–173. doi: 10.1080/02757259409532220

Chang C R, Li M H, Chang S D, 2007. A preliminary study on the local cool-island intensity of Taipei city parks. *Landscape and Urban Planning*, 80(4): 386–395. doi: 10.1016/j.landurbplan.2006.09.005

Chen Yunhao, Li Xiaobing, Shi Peijun *et al*., 2002. Study on spatial pattern of urban heat environment in Shanghai city. *Scientia Geographica Sinica*, 22(3): 317–323. (in Chinese)

Coudert B, Ottlé C, Briottet X, 2008. Monitoring land surface processes with thermal infrared data: Calibration of SVAT parameters based on the optimization of diurnal surface temperature cycling features. *Remote Sensing of Environment*, 112(3): 872–887. doi: 10.1016/j.rse.2007.06.024

Demographia, 2010. Demographia world urban areas & population projections. Available at: http://www.demographia.com/db-worldua.pdf

Geary R C, 1954. The contiguity ratio and statistical mapping. *Incorporated Statistician*, 5(3): 115–141.

Getis A, Ord J, 1992. The analysis of spatial association by distance statistics. *Geographical Analysis*, 24: 189–206. doi: 10.1007/978-3-642-01976-0_10

Golden J, 2004. The built environment induced urban heat island effect in rapidly urbanizing arid regions—A sustainable urban engineering complexity. *Environment Science*, 1(4): 321–349. doi: 10.1080/15693430412331291698

Grimm N B, Faeth S H, Golubiewski N E *et al*., 2008. Global change and the ecology of cities. *Science*, 319(5864): 756–760. doi: 10.1126/science.1150195

Howard L, 1833. *TheClimate of London*, *vols. I–III*. London: Harvey and Dorton.

Imhoff M L, Zhang P, Wolfe R E *et al*., 2010. Remote sensing of the urban heat island effect across biomes in the continental USA. *Remote Sensing of Environment*, 114(3): 504–513. doi: 10.1016/j.rse.2009.10.008

Jiménez-Muñoz J C, Sobrino J A, 2003. A generalized single-channel method for retrieving landsurface temperature from remote sensing data. *Journal of Geophysical Research*, 108 (D22): 4688. doi: 10.1029/2003JD003480.

Jiménez-Muñoz J C, Skobrino J A, 2006. Error sources on the land surface temperature retrieved from thermal infrared single channel remote sensing data. *International Journal of Remote Sensing*, 27(5): 999–1014. doi: 10.1080/ 01431160500075907

Li Shuangcheng, Zhao Zhiqiang, Xie Miaomiao *et al*., 2010. Investigating spatial non-stationary and scale-dependent relationships between urban surface temperature and environmental factors using geographically weighted regression. *Environmental Modelling & Software*, 25(12): 1789–1800. doi: 10.1016/j.envsoft.2010.06.011

Li Weifeng, Wang Yanglin, Peng Jian *et al*., 2005. Landscape spatial changes associated with rapid urbanization in Shenzhen, China. *International Journal of Sustainable Development & World Ecology*, 12(3): 314–325. doi: 10.1080/ 135045005094 69641

Moran P A P, 1948. The interpretation of statistical maps. *Journal of the Royal Statistical Society Series B*, 10(2): 243–251.

Nichol J, Wong M S, 2005. Modeling urban environmental quality in a tropical city, *Landscape and Urban Planning*, 73(1): 49–58. doi: 10.1016/j.landurbplan.2004.08.004

Nichol J, 2009. An emissivity modulation method for spatial enhancement of thermal satellite images in urban heat island analysis. *Photogrammetric Engineering and Remote Sensing*, 75(5): 547–556.

Patz J A, Campbell-Lendrum D, Holloway T *et al*., 2005. Impact of regional climate change on human health. *Nature*, 438(17): 310–317. doi: 10.1038/nature04188

Peng Jian, Wang Yanglin, Ye Minting *et al*., 2007. Effects of land-use categorization on landscape metrics: A case study in urban landscape of Shenzhen, China. *International Journal of Remote Sensing*, 28(21): 4877–4895. doi: 10.1080/01431160601075590

Qin Zhihao, Li Wenjuan, Zhang Minghua *et al.*, 2003. Estimating of the essential atmospheric parameters of mono-window algorithm for land surface temperature retrieval from Landsat TM 6. *Remote Sensing for Land & Resources*, (2): 37–43. (in Chinese)

Rajasekar U, Weng Qihao, 2009. Urban heat island monitoring and analysis using a non-parametric model: A case study of Indianapolis. *ISPRS Journal of Photogrammetry and Remote Sensing*, 64(1): 86–96. doi: 10.1016/j.isprsjprs.2008.05.002

Rosenfeld A H, Akbari H, Bretz S *et al*., 1995. Mitigation of urban heat islands: materials, utility programs, updates. *Energy and Buildings*, 22(3): 255–265. doi: 10.1016/0378-7788(95)00927-P

Roth M, Oke T R, Emery W J, 1989. Satellite-derived urban heat island from three coastal cities and the utilization of such data in urban climatology. *International Journal of Remote Sensing*, 10(11): 1699–1720. doi: 10.1080/01431168908904002

Saaroni H, Ben-Dor E, Bitan A, Potchter O, 2000. Spatial distribution and microscale characteristics of the urban heat island in Tel-Aviv, Israel. *Landscape and Urban Planning*, 48(1–2): 1–18. doi: 10.1016/S0169-2046(99)00075-4

Schott J R, Volchok W J, 1985. Thematic mapper thermal infrared calibration. *Photogrammetric Engineering and Remote Sensing*, 51(9): 1351–1357.

Song Yantun, Yu Shixiao, Li nan *et al*., 2007. Spatial structure of the surface temperature in Shenzhen, China. *Acta Ecologica Sinica*, 27(1): 1489–1498. (in Chinese)

Streutker D R, 2002. A remote sensing study of the urban heat island of Houston, Texas. *International Journal of Remote Sensing*, 23(13): 2595–2608. doi: 10.1080/01431160110115023

Streutker D R, 2003. Satellite-measured growth of the urban heat island of Houston, Texas. *Remote Sensing of Environment*, 85(3): 282–289. doi: 10.1016/S0034-4257(03)00007-5

Tobler W R, 1970. A computer movie simulating urban growth in the Detroit region. *Economic Geography*, 46: 234–240.

Valor E, Caselles V, 1996. Mapping land surface emissivity from NDVI: Application to European, African, and South American

Areas. *Remote Sensing of Environment*, 57(3): 167–184. doi: 10.1016/0034-4257(96)00039-9

Voogt J A, 2002. Urban heat island. In: Ian Douglas (ed.). *Encyclopedia of Global Environmental Change*. Chichester: John Wiley & Sons, Ltd: 660–666.

Voogt J A, Oke T R, 2003. Thermal remote sensing of urban climates. *Remote Sensing of Environment*, 86(3): 370–384. doi: 10.1016/S0034-4257(03)00079-8

Wang Fuhai, 2003. *Study on the Dynamic Process of Spatial Extension in the City of Shenzhen*. Beijing Peking University, China. (in Chinese)

Wang J F, 2006. *Spatial Analysi*s. Beijing: Science Press. (in Chinese)

Weng Qihao, Yang Shihong, 2004. Managing the adverse thermal effects of urban development in a densely populated chinese city. *Journal of Enviromental Management*, 70(2): 145–156. doi: 10.1016/j.jenvman.2003.11.006

Weng Qihao, Liu Hua, Liang Bingqing *et al*., 2008. The spatial variations of urban land surface temperatures: pertinent factors, zoning effect, and seasonal variability. *IEEE Journal of Selected Topics in Applied Earth Observations and Remote Sensing*, 1(2): 154–166. doi: 10.1109/JSTARS.2008.917869

Weng Qihao, 2003. Fractal analysis of satellite-detected urban heat island effect. *Photogrammetric Engineering & Remote Sensing*, 69(5): 555–566.

Wukelic G E, Gibbons D E, Martucci L M *et al*., 1989. Radiometric calibration of landsat thematic mapper thermal band. *Remote Sensing of Environment*, 28, 339–347. doi: 10.1016/0034-4257(89)90125-9

Xie Miaomiao, Zhou Wei, Wang Yanglin *et al*., 2008. Thermal environment effect of land use in urban area: A case study in Ningbo urban area. *Acta Scientiarum Naturalium Universitatis Pekinensis*, 44(5): 815–821. (in Chinese)

Yuan F, Bauer M E, 2007. Comparison of impervious surface area and normalized difference vegetation index as indicators of surface urban heat island effects in Landsat imagery. *Remote Sensing of Environment*, 106(3): 375–386. doi: 10.1016/j.rse.2006.09.003

Yue Wenze, Xu Lihua, 2007. Thermal environment effect of urban land use type and pattern: A case study of central area of Shanghai City. *Scientia Geographica Sinica*, 27(2): 243–248. (in Chinese)

Yue Wenze, Xu Jianhua, 2008. Impact of human activities on urban thermal environment in Shanghai. *Acta Geographica Sinica*, 63(3): 247–256. (in Chinese)

Zhang Chao, Yang Binggeng, 1991. *Quantitative Geography* (*Second edition*). Beijing: Higher Education Press: 50–54. (in Chinese)

Zhang Xiaofei, Wang Yanglin, Wu Jiansheng *et al*., 2006. Study on land surface temperature vegetation cover relationship in urban region: A case in Shenzhen City. *Geographical Research*, 25(3): 369–377. (in Chinese)

Zhou Yixing, 1995. *Urban Geography*. Beijing: The Commercial Press. (in Chinese)